14:17:47 OCA PAD AMENDMENT - PROJECT HEADER INFORMATION 04/29/97

Active

Project #: E-20-M10 Cost share #: Rev #: 3
Center # : 10/24-6-R8809-0A0 Center shr #: OCA file #:
Work type : RES
Contract#: AGMT DTD 960130 Mod #: 2 Document : CONT
Prime #: Contract entity: GTRC

Subprojects ? : N CFDA: N/A
Main project #: PE #: N/A

Project unit: CIVIL ENGR Unit code: 02.010.116
Project director(s):
ROBERTS P J W CIVIL ENGR (404)894-2219

Sponsor/division names: INSTIT OF PAPER & SCI TEC INC / ATLANTA, GA
Sponsor/division codes: 500 / 152

Award period: 951110 to 970630 (performance) 970630 (reports)

Sponsor amount	New this change	Total to date
Contract value	15,641.00	69,703.00
Funded	15,641.00	69,703.00
Cost sharing amount		0.00

Does subcontracting plan apply ?: N

Title: "EXPERIMENTAL STUDIES OF HEADBOX FLOW"

PROJECT ADMINISTRATION DATA

OCA contact: Anita D. Rowland 894-4820

Sponsor technical contact	Sponsor issuing office
CYRUS AIDUN	MARSHA MCCLATCHY
(404)894-6645	(404)894-1494
THE INSTITUTE OF PAPER SCIENCE & TECHNOLOGY	THE INSTITUTE OF PAPER SCIENCE & TECHNOLOGY
500 10TH ST., NW	500 10TH ST., NW
ATLANTA, GA 30318	ATLANTA, GA 30318
ATTN: ENGINEERING & PAPER MATLS. DIV	

Security class (U,C,S,TS) : U ONR resident rep. is ACO (Y/N): Y
Defense priority rating : N/A N/A supplemental sheet
Equipment title vests with: Sponsor X GIT
PER M. MCCLATCHY ON 3/1/96 TITLE VESTS W/IPST. AGRMNT IS SILENT ON THIS ISSUE
Administrative comments -
AMEND 2 ADDS INCREMENTAL FUNDS.

PROJECT CLOSEOUT - NOTICE

Closeout Notice Date 24-OCT-1997

Project Number E-20-M10 Doch Id 40015

Center Number 10/24-6-R8809-0A0

Project Director ROBERTS, PHILIP

Project Unit CIVIL ENGR

Sponsor INSTIT OF PAPER & SCI TEC INC/ATLANTA, GA

Division Id 6077

Contract Number AGMT DTD 960130 Contract Entity GTRC

Prime Contract Number

Title "EXPERIMENTAL STUDIES OF HEADBOX FLOW"

Effective Completion Date 30-JUN-1997 (Performance) 30-JUN-1997 (Reports)

Closeout Action:	Y/N	Date Submitted
Final Invoice or Copy of Final Invoice	Y	
Final Report of Inventions and/or Subcontracts	N	
Government Property Inventory and Related Certificate	N	
Classified Material Certificate	N	
Release and Assignment	N	
Other	N	

Comments

Distribution Required:	
Project Director/Principal Investigator	Y
Research Administrative Network	Y
Accounting	Y
Research Security Department	N
Reports Coordinator	Y
Research Property Team	Y
Supply Services Department	Y
Georgia Tech Research Corporation	Y
Project File	Y

E-20-M10

#1

Experimental Studies of Headbox Flow

Project E20-M10

Final report

Period: 10/11/95 to 6/30/96

The prototype, full size, headbox was installed in the test facility in the Hydraulics Laboratory at the School of Civil Engineering at Georgia Tech. This facility consists of a high flowrate pump, flow meter, and associated plumbing. The flow meter was calibrated by a weighing tank method and the flow system is now operational. A new laser was purchased for the Laser Doppler Anemometer (LDA) and a portable carriage system was fabricated to allow use of the LDA in the test facility. A special traversing mechanism was built to allow use of the fiber optic probe head near to the jet. Preliminary measurements with the LDA of velocity and turbulence profiles in the jet were made. The test facility and LDA are now fully operational and ready for the detailed measurements to be made in the second year of the project beginning July 1, 1996.

E-20-M10
#2

Headbox Hydrodynamic Analysis and LDV Measurements

By Philip J. W. Roberts and Agnes Kovacs

1. Introduction

The turbulence characteristics of the flow in headboxes are of great importance to the pulp and paper industry. It has a major influence on the quality and uniformity of the paper produced. The flow entering the headbox has a 3% concentration of paper fibers. It is important that these fibers remain in suspension and are oriented in the same direction when they leave the headbox. The fiber orientation in the jet at the headbox exit is dependent on the three-dimensional flow in the headbox. To optimize the headbox design it is vital to know the details of this flow. A major objective of optimization is to minimize secondary flows.

The objectives of this project are to (1) investigate the characteristics of the flow in the headbox using accurate laser Doppler velocimeter (LDV) measurements, and (2) to explore methods of enhancing the turbulence level for better fiber dispersion and paper and board formation. The results of the LDV measurements are presented in this report. The methods of enhancing turbulence levels are discussed in a separate report.

In this report, we describe the experimental procedures used, present the results, and summarize the conclusions. An analysis of the flow in a converging channel similar to that occurring in a headbox is presented in Appendix A. In this Appendix the governing equations and their similarity solution is discussed.

2. Apparatus

The LDV measurements were made in a full size prototype headbox test facility installed in the Hydraulics Laboratory at the School of Civil Engineering at Georgia Tech. This facility consists of a high flowrate pump, flow meter, and associated plumbing. The flowmeter was calibrated with a weighing tank. A photograph of the operating system is shown in Figure 1.

The LDV is a one-component system fiber optic system manufactured by Aerometrics. A schematic diagram showing the experimental configuration is shown in Figure 2. The system works in backscatter mode with velocity computed via a Frequency domain signal processor. It was found that no artificial seeding of the flow was necessary, with natural seeding present in the water supply providing data rates usually exceeding 100 Hz. The laser was a 1 Watt Lexel laser. A portable system was fabricated to allow use of the LDV in the test facility. A special traversing mechanism was built to allow use of the fiber optic probe head (transceiver) near to the jet and to measure its precise location. A second traversing mechanism was built to allow measurement of velocities inside the headbox.

3. Results

Two sets of experiments were done to measure velocities at the jet exit and in the headbox. Both sets of experiments were done with and without the guide sheets in place. All measurements were done at a flowrate of 50.5 L/s ± 3% (800 gpm) with a jet opening of 12.7 mm (0.5 inch). The jet width is 406 mm (16 inches) so the average jet velocity at the exit was 9.8 m/s. The headloss in the headbox was somewhat higher with the sheets installed than without them.

3.1 Measurements at the Jet Exit

Vertical profiles of the variation of the horizontal streamwise, u, and cross-flow velocity, v, at the jet exit were made at five horizontal locations as shown in Figure 3. The horizontal locations were at $y = 2$, 4, 8, 12, and 14 inches. The vertical coordinate, z, of the point of measurement is the distance from the Lucite attached to the lower surface of the slice. The laser probe is placed below the Lucite looking upwards as shown in Figure 2. Three measurements were recorded at each location. Data were obtained both with the separating plastic sheets inside the headbox and with them removed.

The mean streamwise and cross-flow velocities are shown in Figures 4 and 5. Typical streamwise velocities are greater then the average velocity at the jet exit due to the vena contracta effect. It can be seen that the streamwise velocity is not exactly uniform. It is more uniform with the sheets. In this case, the variation of velocity over the cross section is about ± 3% of the mean value. Without the sheets the variation is almost ± 10%. The results also imply some asymmetry of the flow about the jet exit centerline. The flow closer to the headbox inlet (y = 14 inches) is less uniform than farther away (y = 2 inches).

The cross-flow velocity is very small, essentially zero, with the sheets installed, implying essentially straight streamlines parallel to the headbox axis with negligible secondary circulations. The magnitudes are substantially higher without the sheets. For this case, the velocities are generally negative to the left of the headbox centerline, and positive to the right. This implies diverging flow to the headbox walls. At the far wall (y = 14 inches) especially, the velocities are negative near the free surface and positive near the middle and lower boundary. This implies a rather strong secondary circulation within the jet, which is suppressed by the sheets.

The streamwise and crossflow variations of turbulence intensity (proportional to the normal Reynolds stresses) are shown in Figures 6 and 7. They are shown as the magnitude of the root mean square (rms) value of the velocity fluctuations about the local mean value.

The rms of the streamwise velocity is smaller and more uniform with the sheets than without. Typical streamwise values with the sheets are about 0.3 to 0.6 m/s, corresponding to relative turbulence intensities of about 3 to 6 %. The crosswise rms values are smaller, indicating that the turbulence is not isotropic. Without the sheets the rms values are higher and less uniform. Streamwise turbulence intensities are typically 10 % or greater and is higher near the lower boundary and at the free surface.

3.1 Measurements in the Headbox

Measurements of the streamwise, u, and vertical velocity, w, were made inside the headbox along the longitudinal axis. The measurements were made at a distance $y = 3''$ from the Lucite wall along the centerline of the headbox. The longitudinal variations of the mean streamwise and vertical velocities are shown in Figure 8. The corresponding rms values of the velocity fluctuations are shown in Figure 9.

The streamwise velocity increases along the headbox due to the tapering cross section. Without the sheets the streamwise velocity is larger near the tube and smaller near the slice than with the sheets. With the sheets the velocity increases more uniformly along the headbox. The vertical velocities with the sheets are very small. With the sheets, the vertical velocity is quite strong, up to about 1.8 m/s near the inlet tube bank. This velocity is positive, i.e. upwards. It is also positive near the jet exit but with a much smaller magnitude, about 0.1 m/s.

The streamwise rms intensities are smaller with the sheets installed than without them. This is particularly true near to the inlet tube bank, where typical rms values are about twice as large without the sheets. This difference decreases with distance along the headbox until the jet exit, where the rms values are very close.

The relative turbulence decreases rapidly with distance along the headbox. With the sheets, it from about 40 % near the tube bank to about 3 % near the jet exit. The high values near the inlet tubes are presumably due to the shear induced by the individual jets issuing from the tubes. This turbulence decays with distance until by the jet exit it has been replaced by turbulence due to shear at the top and bottom boundaries of the headbox, with typical values around 3 %.

4. Conclusions

1) The streamwise velocity of the flow leaving the headbox at the jet exit is more uniform with the sheets.

2) The cross-flow velocities are very small with the sheets. This indicates the secondary circulations are virtually eliminated by the sheets.

3) Cross flow velocities without the sheets can be quite substantial and spatially variable without the sheets. This indicates the presence of secondary circulations.

4) The magnitude of the turbulent fluctuations (expressed as their rms values) are smaller and more spatially uniform over the jet exit with the sheets than without. Relative turbulence intensities over the jet exit are typically about 3 to 6 % with the sheets and are larger without.

5) The streamwise velocity inside the headbox increases more uniformly with the sheets than without them. Vertical velocities in the headbox are essentially eliminated by the sheets but can be quite large without them.

6) With the sheets, the relative turbulence intensity decreases rapidly with distance inside the headbox. It is about 40 % near the inlet tubes and about 3 % near the jet exit. This is presumably due to the decay of the turbulence intensity associated with the multiple inlet jets.

Appendix A: Flow in a Converging Channel

The headbox is an important integral part of paper formation. From the hydrodynamic point of view it is a converging channel. Figure 1a shows the simplified geometry of a headbox. In this converging channel, we consider a two-dimensional high Reynolds' number flow between the two plane walls at $x_2 = 0$ and at $x_2 = x_1 \tan \alpha$. There is a narrow slit (slice) near the origin through which fluid is extracted. Inside the headbox we can assume that the flow divides into an essentially inviscid mainstream with thin viscous boundary layers on the walls, as indicated in Figure 1a.

The similarity solution presented herein follows the analysis of Goldstein (1938) and Acheson (1990). The exact 2-D governing equations are given by

$$u\frac{\partial u}{\partial x_1} + v\frac{\partial u}{\partial x_2} = -\frac{1}{\rho}\frac{\partial p}{\partial x_1} + \nu\left(\frac{\partial^2 u}{\partial x_1^{\,2}} + \frac{\partial^2 u}{\partial x_2^{\,2}}\right)$$

$$u\frac{\partial v}{\partial x_1} + v\frac{\partial v}{\partial x_2} = -\frac{1}{\rho}\frac{\partial p}{\partial x_2} + \nu\left(\frac{\partial^2 v}{\partial x_1^{\,2}} + \frac{\partial^2 v}{\partial x_2^{\,2}}\right) \qquad (1)$$

$$\frac{\partial u}{\partial x_1} + \frac{\partial v}{\partial x_2} = 0$$

where u and v are the velocity components in the x_1 and x_2 directions, respectively. p is the pressure, ρ is the fluid density and ν denotes the kinematic viscosity. The boundary conditions at the walls are u=v=0. The inviscid outer flow is purely radial, i.e.

$$(r) = \frac{Q}{2r\pi}\frac{360}{\alpha} = \frac{q}{r} \qquad (2)$$

where the flow rate Q is constant and positive and q is introduced to ease the derivation. Since, we want to analyze the boundary layer or inner layer near the wall at y=0 the radial accelerating outer flow becomes $U(x) = q/x_1$. In the outer region the pressure distribution comes from

$$\frac{\partial U}{\partial x_1} = -\frac{1}{\rho}\frac{\partial p}{\partial x_1} \qquad (3)$$

Substituting the above favorable pressure gradient into the 2-D boundary layer momentum equation

$$u\frac{\partial u}{\partial x_1} + v\frac{\partial u}{\partial x_2} = -\frac{1}{\rho}\frac{\partial p}{\partial x_1} + \nu\frac{\partial^2 u}{\partial x_1^{\,2}} \qquad (4)$$

we obtain

$$u\frac{\partial u}{\partial x_1}+v\frac{\partial u}{\partial x_2}=-\frac{q^2}{x_1^{\,3}}+\nu\frac{\partial^2 u}{\partial x_1^{\,2}} \tag{5}$$

In the similarity solution u is assumed to be

$$u=-\frac{q}{x_1}f'(\eta) \tag{6}$$

where $\eta = y/g(x_1)$ and $g(x)= x_1 \sqrt{(\nu/q)}$. This implies that the mainstream boundary condition for the inner flow is $f'(\infty)=0$. A streamline representation of the flow field yields the other velocity component so

$$v=-\frac{q^{1/2}\nu^{1/2}}{x_1}\eta f'(\eta) \tag{7}$$

which satisfies v=0 on $x_2=0$. Substituting the velocity components (6) and (7) into equation (5) we obtain

$$f'^2=1+f''' \tag{8}$$

The no-slip condition u=0 on $x_2=0$ is satisfied provided that $f'(0)=0$. Substituting $F(\eta) = f'(\eta)$ a second-order problem is defined by

$$F''+1-F^2=0 \tag{9}$$

which is subject to boundary conditions; $F(0)=0$ and $F(\infty)=1$. Integration of equation (9) and the application of the boundary conditions lead to the following solution

$$F(\eta)=-2+3\tan^2\left(\frac{\eta}{\sqrt{2}}+1.14\right) \tag{10}$$

The boundary layer thickness along the wall is proportional to the distance from the origin, i.e.

$$\delta \propto x_1\sqrt{\frac{\nu}{q}} \tag{11}$$

It is increasing with distance from the origin. This boundary layer is thin if $q/\nu>>1$.

The above detailed analysis demonstrates the dynamics of headbox flows. However, it has ignored several of its important features. The boundary layer in headboxes is a turbulent boundary layer that cannot be characterized with one constant turbulent viscosity value ν along the wall. The structure of this turbulent boundary layer has been the subject of extensive research but it is still not well understood. The governing equations of turbulent boundary layers and their numerical solutions are summarized e.g. in the book of Cebici and Bradshaw (1984).

The Reynolds equation for the turbulent boundary layer is given by

$$u\frac{\partial u}{\partial x_1}+v\frac{\partial u}{\partial x_2}=-\frac{q^2}{x_1^3}+\frac{1}{\rho}\frac{\partial}{\partial x_1}(\mu\frac{\partial u}{\partial x_1}+\tau^{x_1x_2}) \tag{12}$$

where $\tau^{x_1x_2}$ is a turbulent Reynolds stress and μ is the dynamic molecular viscosity. The similarity solution may be assumed in the form in a form of the logarithmic law of the wall

$$\frac{u}{u_*}=f(y^+)+\frac{\Pi w(\eta)}{\kappa} \tag{13}$$

as suggested by Cole (1956). $u_* = \sqrt{(\tau/\rho)}$ is the shear velocity and κ (~ 0.4) is known as the von Karman constant. $\eta = x_2/\delta$ denotes the boundary layer coordinate, where $\delta=\delta(x_1)$ is the boundary layer thickness. $y^+ = x_2 u_*/\upsilon$ is known as the wall variable. $f(y^+)$ represents the logarithmic portion of the near wall flow for $y^+ > 30$:

$$f(y^+)=\frac{1}{\kappa}\ln y^+ + A \tag{14}$$

$w(\eta)$ is Cole's wake function which for a wide class of flows may be approximated by

$$w(\eta)=1-\cos\eta\pi \tag{15}$$

In the above equations A and Π are constants whose value are determined from experiments. A is a function of flow conditions e.g. A can be set to about 5.5 for turbulent flow over smooth boundary. Cole's wake strength coefficient Π depends on the flow geometry and pressure gradient e.g. Π=0.55 for zero pressure gradient flat-plate boundary layer. Adjacent to the wall, the very thin viscous sublayer occupies about 1% of the boundary layer thickness.

Approximation of the flow with two-dimensional outer and inner layer solutions does not provide the details of the velocity field. Secondary flows in the plains normal to the main flow cannot be simulated by the above given solutions. Beyond these details, flows in headboxes have significantly more complex geometry and at the slice free surface boundary conditions. Among these circumstances there are two ways to investigate headbox flows. Computational fluid dynamics can solve the complete governing equations or experiments can be carried out to measure the flow field. This study presents the results of an LDV experiment.

References:

Goldstein, S. (1938) *Modern developments in fluid dynamics*. Dover, New York ,1965.

Acheson, D.J. (1990) *Elementary fluid dynamics*. Clarendon Press, Oxford 1990.

Coles, D. (1956) The law of the wake in the turbulent boundary layer. *J. Fluid Mech. 1*, 191-226.

Cebici, T. and Bradshaw, P. (1984) *Physical and computational aspects of convective heat transfer*. Springer-Verlag, New York 1988.

Appendix B. Supplemental Velocity Records Obtained in the Headbox

Two sets of measurements were taken inside the headbox without sheets installed. The first one is for 780 gallon/min, the second one is for 802 gallon/min. These records are provided on separate files. The locations of the measurements are shown in Figure B1. The nomenclature for these data series is shown in Table B1.

Table B1. File Names for Supplemental Data

Number	x (inches)	y (inches)		
		2	2.5	3
1	-2	u20.112 v20.112	u15.112 v15.112	u10.112 v10.112
2	-3	u20.111 v20.111	u15.111 v15.111	u10.111 v10.111
3	-4	u20.110 v20.110	u15.110 v15.110	u10.110 v10.110
4	-25	u20.89 v20.89	u15.89 v15.89	u10.89 v10.89
5	-26	u20.88 v20.88	u15.88 v15.88	u10.88 v10.88
6	-27	u20.87 v20.87	u15.87 v15.87	u10.87 v10.87

The first column refers to the location of these records on Figure B1. Data sampling rate for these cases is equal to or greater than 100Hz.

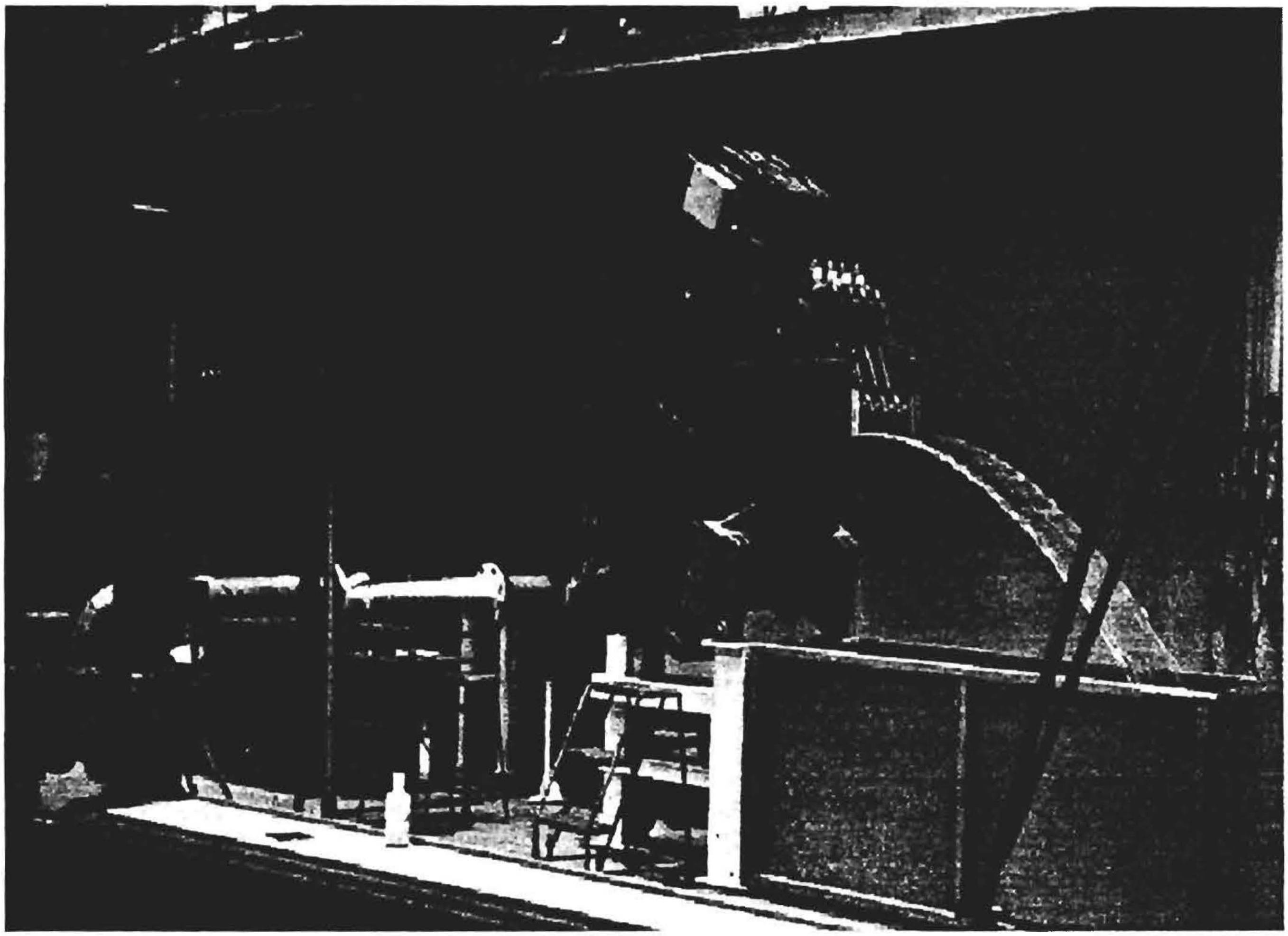

Figure 1. Photograph of Headbox Experimental Configuration

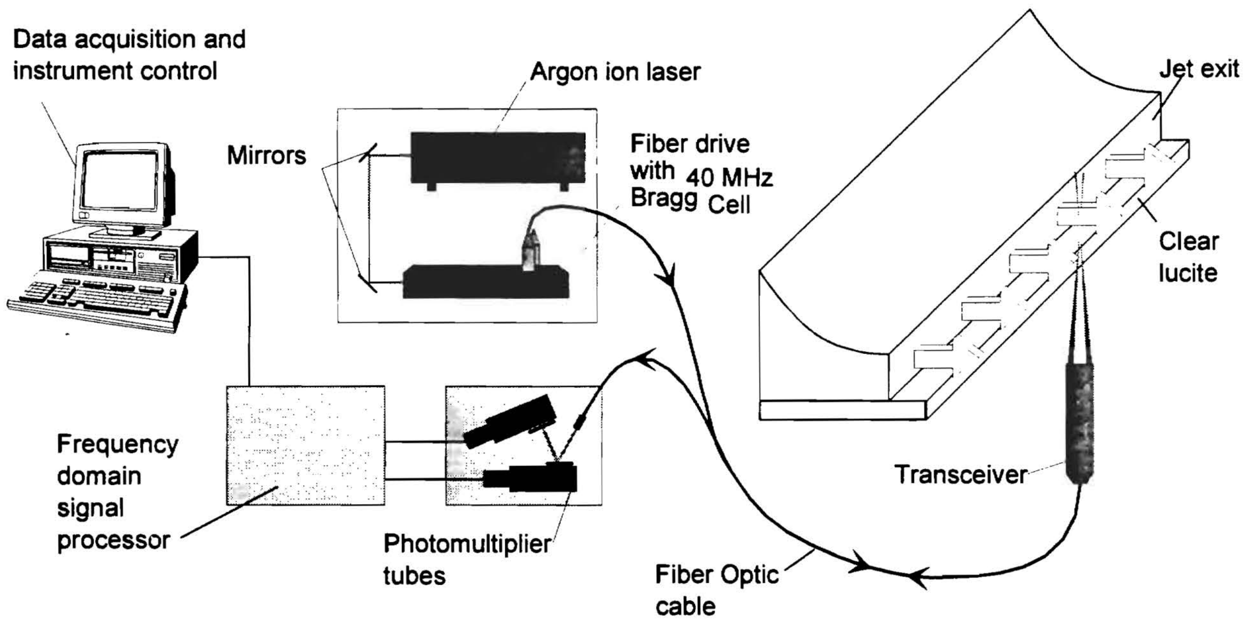

Figure 2. Schematic Depiction of LDV Experimental Configuration

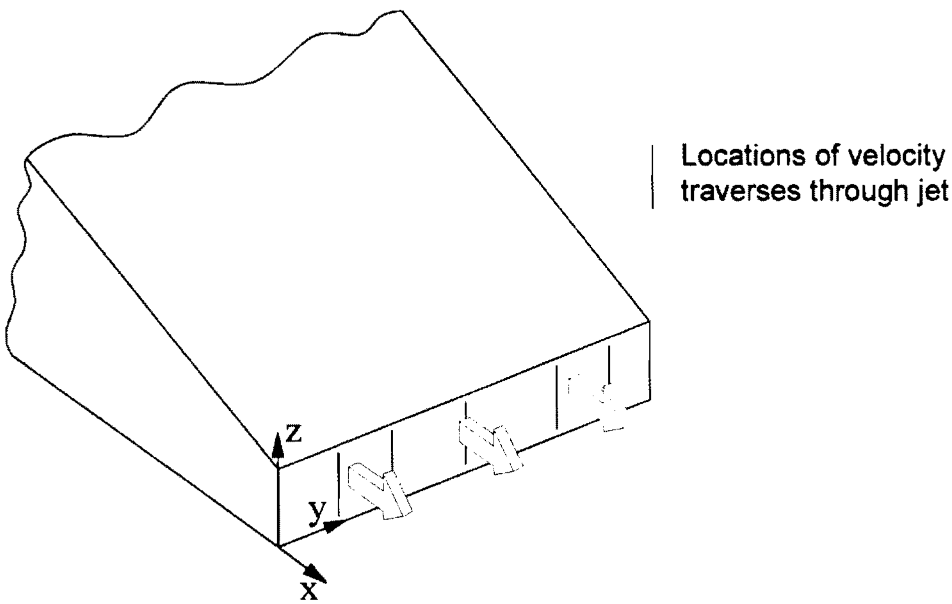

Figure 3. Coordinate System Used for Velocity Measurements

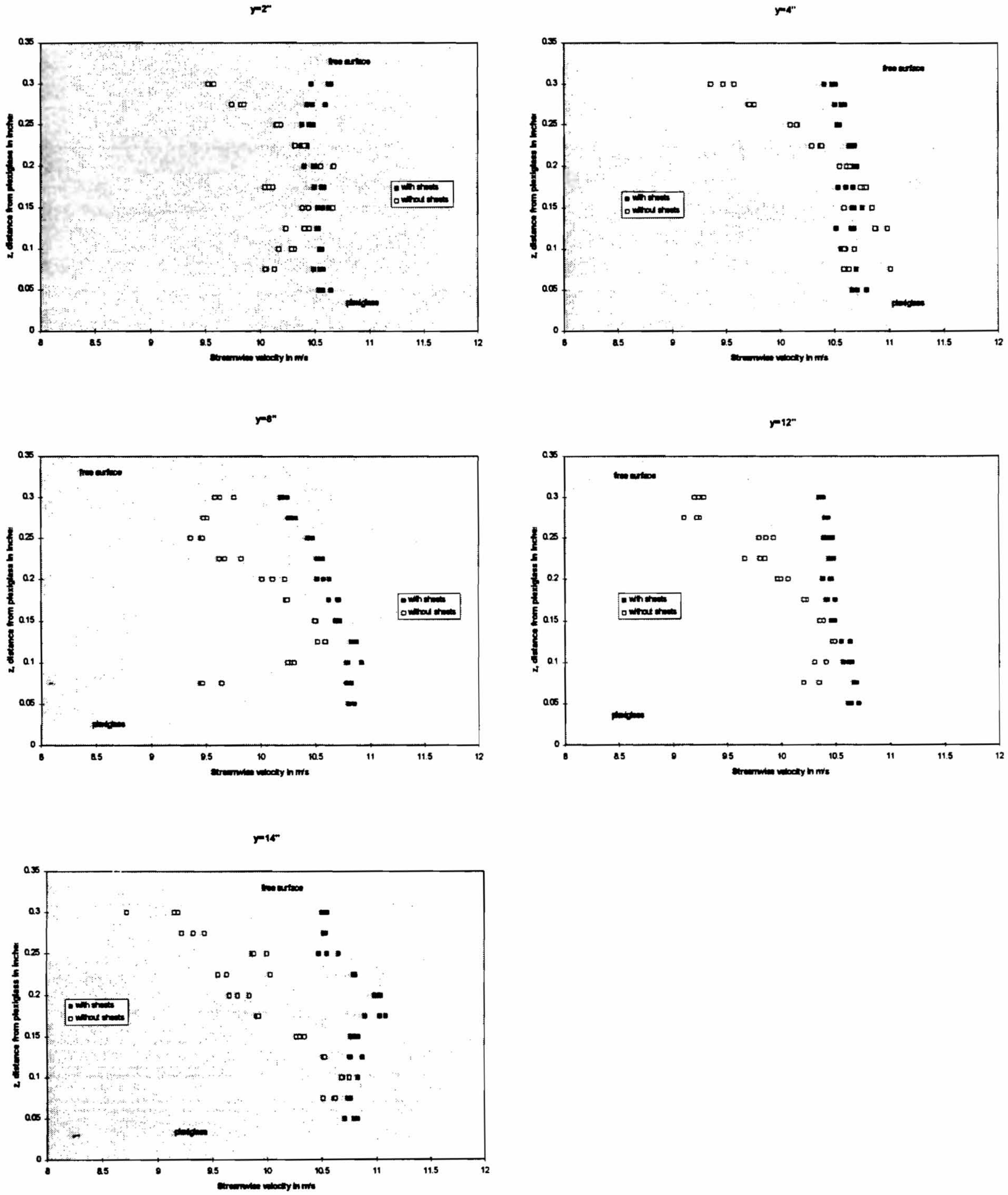

Figure 4. Mean Streamwise Velocity, u at the Jet Exit. With and Without Sheets.

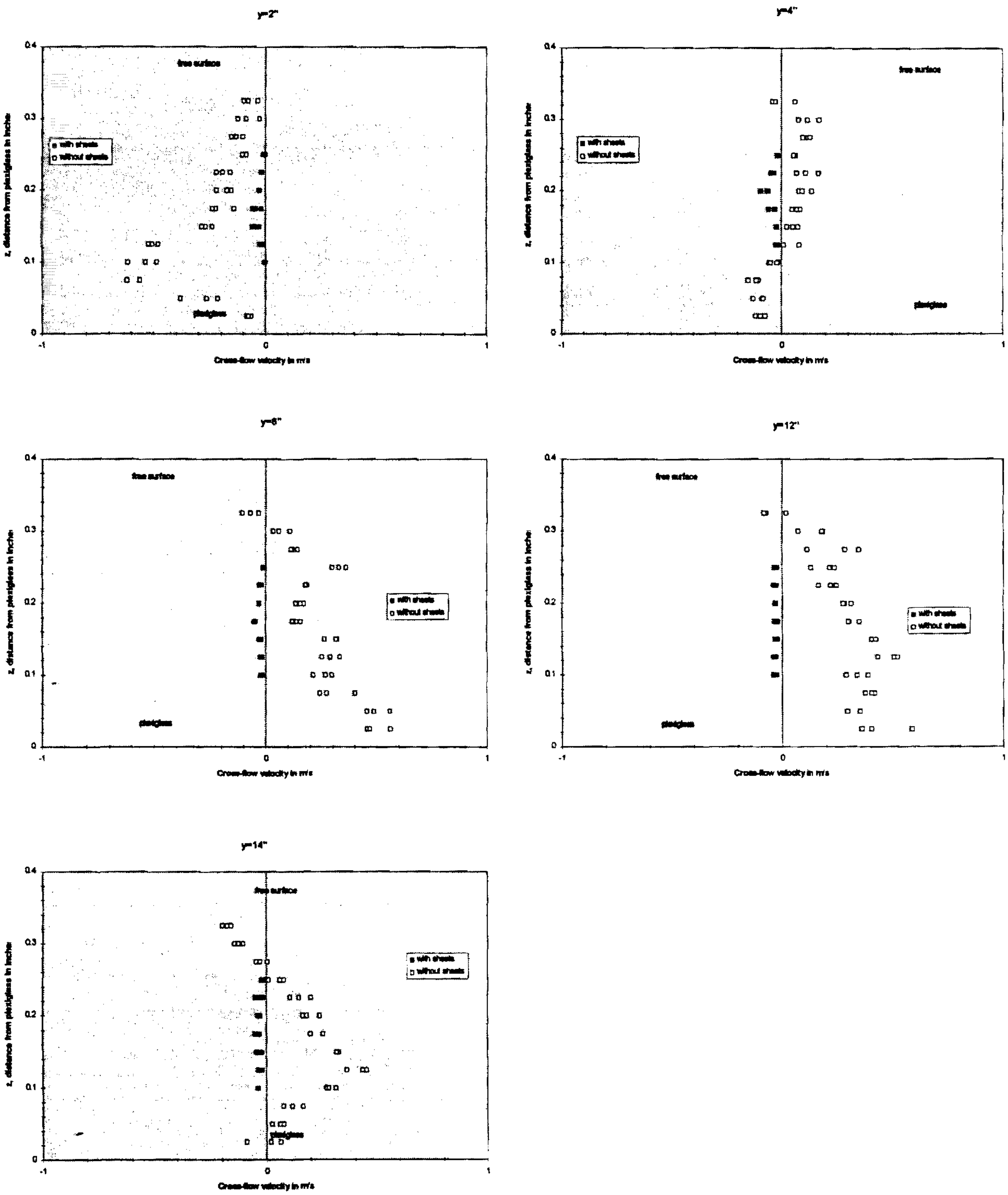

Figure 5. Mean Crossflow Velocity, v at the Jet Exit. With and Without Sheets.

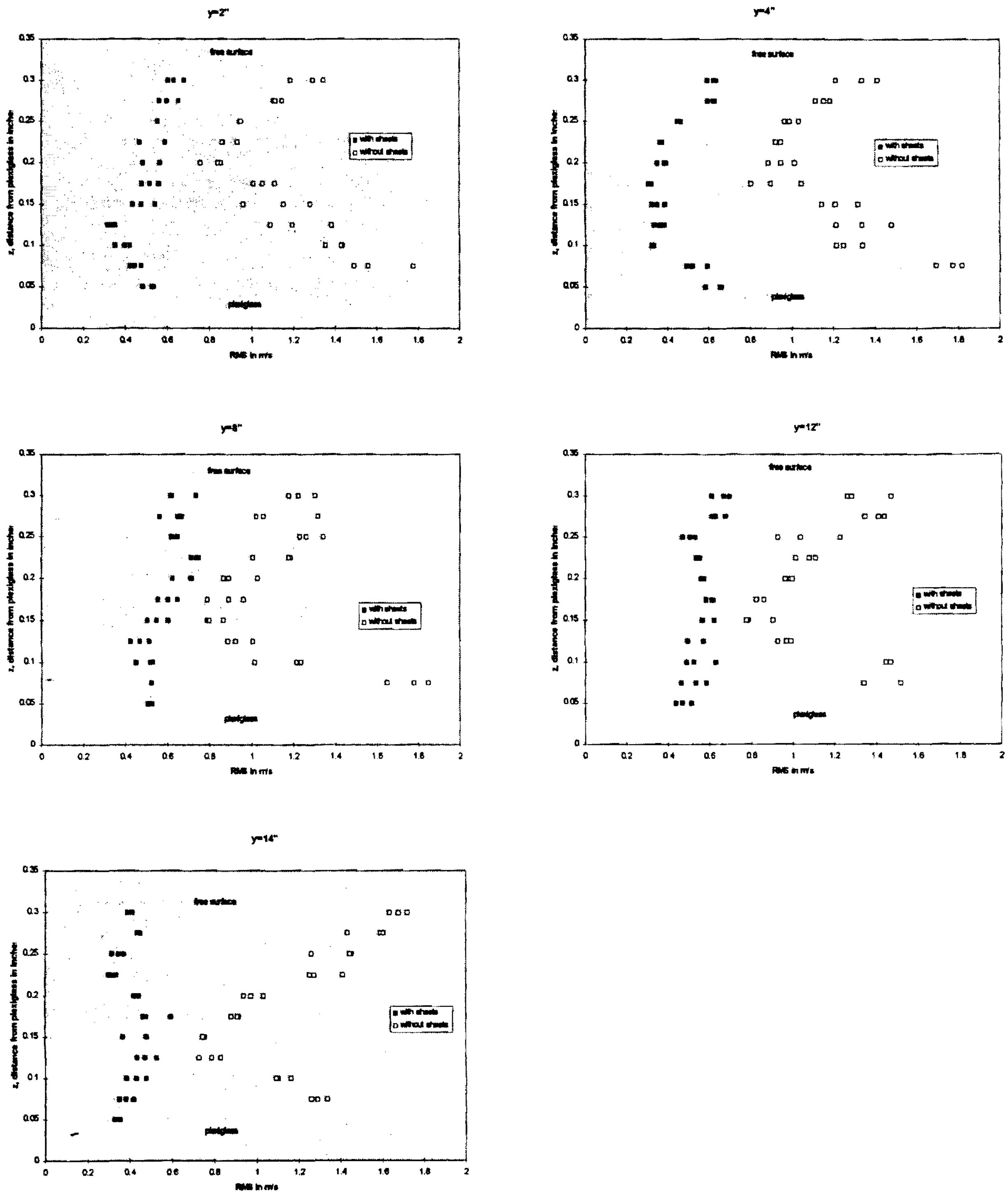

Figure 6. rms of Streamwise Velocity, u' at the Jet Exit. With and Without Sheets.

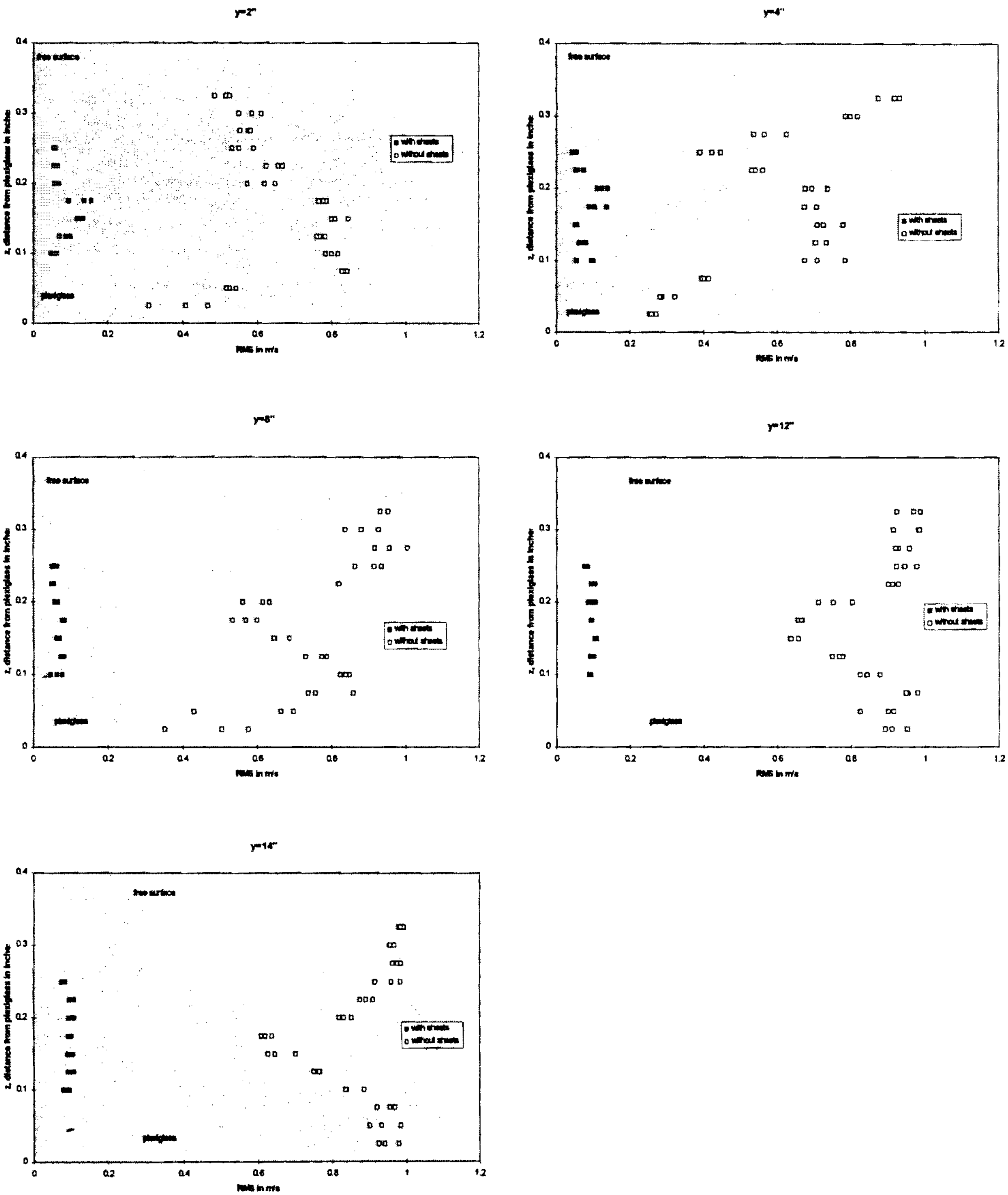

Figure 7. rms Crossflow Velocity, v' at the Jet Exit. With and Without Sheets.

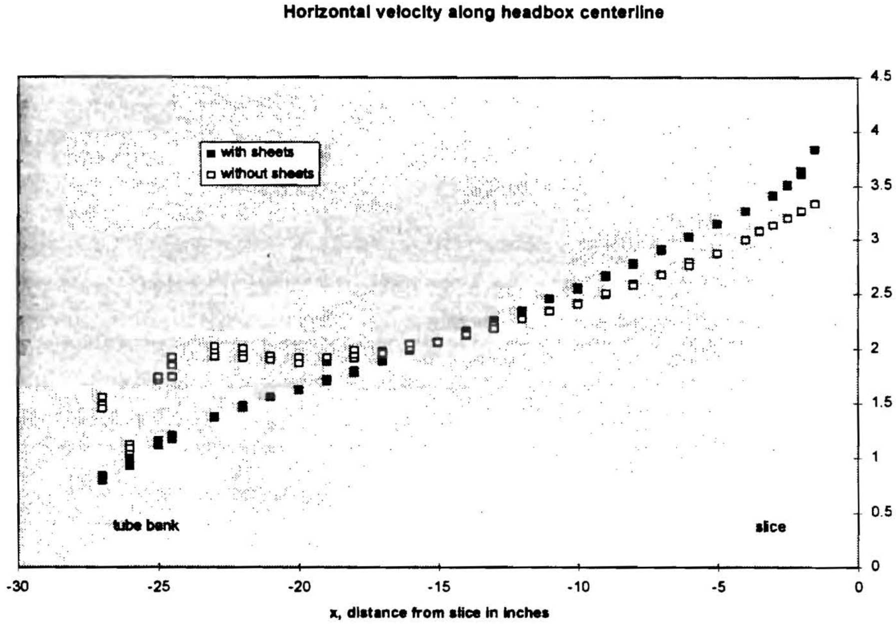

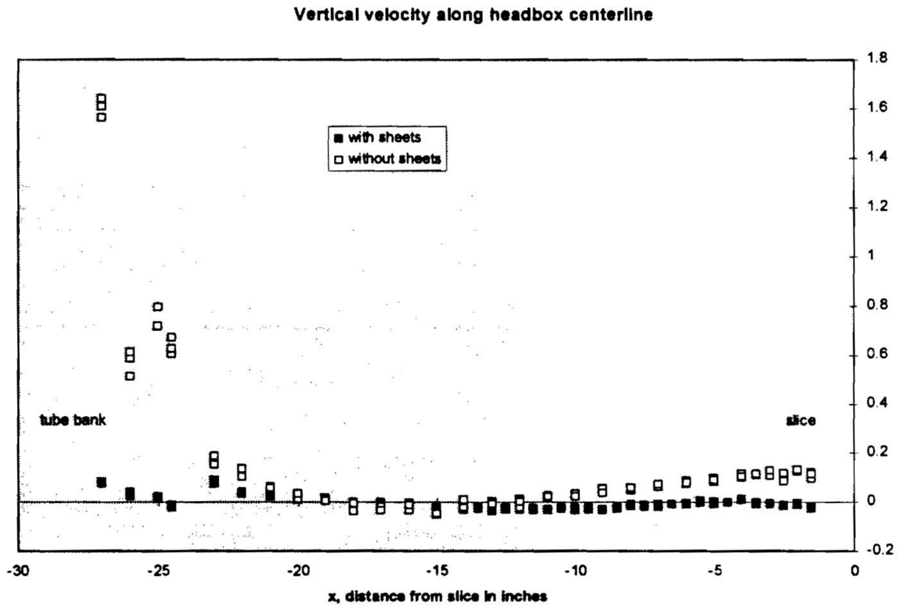

Figure 8. Mean Streamwise Velocity, u, and Vertical Velocity, v, Along Headbox Centerline

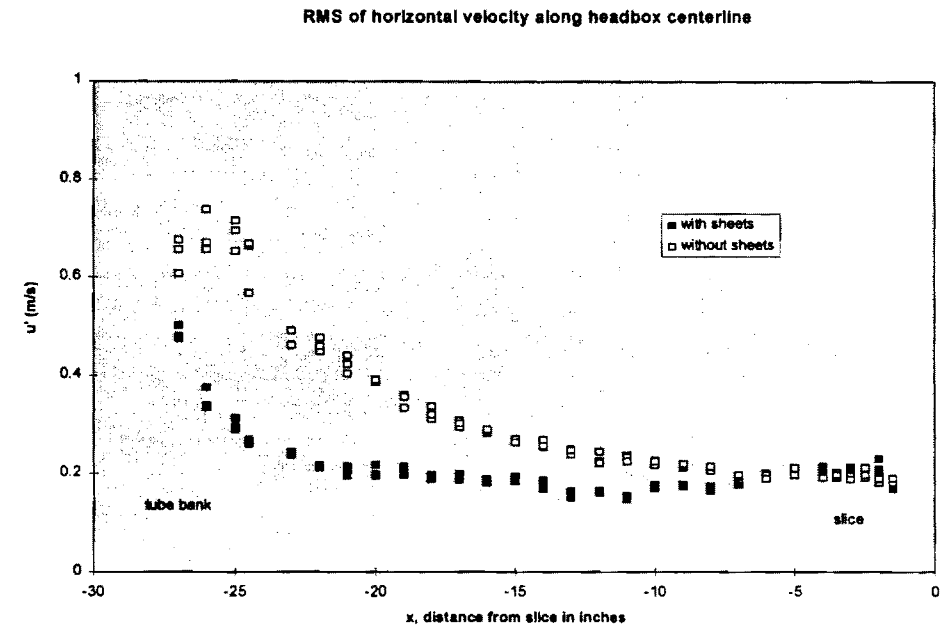

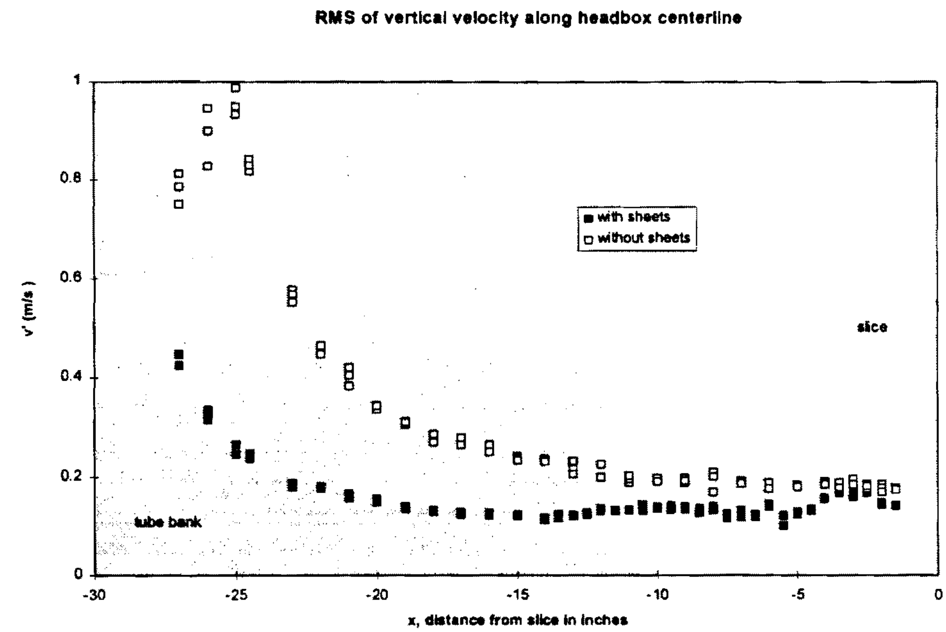

Figure 9. rms Streamwise Velocity, u', and Vertical Velocity, v', Along Headbox Centerline

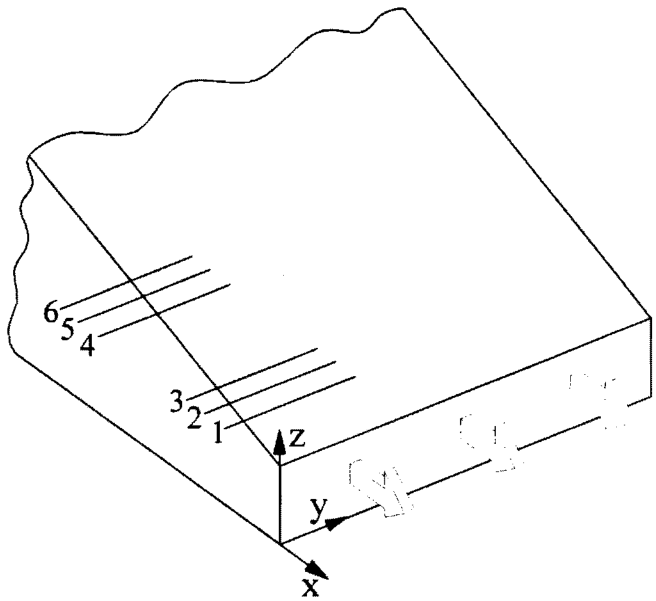

Figure B1. Locations of Supplemental Velocity Measurements